ICIC Express Letters
Volume **11**, Number **10**, October **2017**
 ISSN 1881-803X
pp. **1555–1561**

ADAPTIVE COMMAND-FILTERED BACKSTEPPING CONTROL FOR PHOTOVOLTAIC GRID-CONNECTED INVERTER

Gang Wang, Wenxu Yan, Dezhi Xu, Xiaoqi Song and Yujin Hong

Institute of Electrical Engineering and Intelligent Equipment
School of Internet of Tings Engineering
Jiangnan University
No. 1800, Lihu Ave., Wuxi 214122, P. R. China
lutxdz@126.com

Received April 2017; accepted July 2017

Abstract. *This paper proposes a nonlinear control strategy to adjust the DC link voltage and the current to control the amount of injected power into the grid. The controller is projected using an adaptive backstepping technique in consideration of the uncertain part and the external disturbance of actual application of the system. In order to solve the problems of differential expansion and the control saturation, a command filter is employed to eliminate the impact of time derivative and control saturation. The overall stability of the whole system is analyzed based on the Lyapunov functions. Simulation results indicate good dynamic and static performance and strong robustness with the proposed controller.*
Keywords: PV, Grid-connected inverter, Adaptive backstepping, Command filter

1. **Introduction.** Renewable energy Sources (RESs), especially wind and solar, for several reasons, are compared with traditional energy sources, in recent years to obtain more power generation opportunities. In addition, power generation from photovoltaic systems is supported by governments and many industries, primarily to encourage the reduction of carbon emissions and environmental pollution. Although the photovoltaic system can be installed in two ways: stand-alone and grid-connected, about 98 percent of the photovoltaic systems are built in grid-connected system [1].

Some examples of nonlinear controllers for photovoltaic grid-connected system include model predictive controller [2], sliding-mode controllers [3], and feedback linearizing controllers [4]. A nonlinear backstepping controller is designed in [5] which overcomes some limitations of feedback linearizing controller by considering all nonlinearities of the system. However, the traditional backstepping requires that exact information of the model is obtained and the parameter uncertainties are not taken into consideration [6].

In order to ensure the stability of most control systems with nonlinearities and parameter uncertainties, adaptive backstepping approach has been investigated, which has been proved to be effective to achieve the satisfactory control performance [7]. However, it is not perfect because of the derivative of the virtual control and the control saturation problem. At present, there are many methods to solve the above-mentioned defects such as dynamic surface control [8] and command-filtered method [9], and among them command-filtered backstepping is a more effective way compared to dynamic surface control [10]. And among them command-filtered backstepping is a more effective method compared with dynamic surface control. Dynamic surface control uses the filter to solve the differential expansion problem. However, the command-filtered backstepping controller can solve the problem of differential expansion, and it can also achieve the asymptotic tracking of the closed-loop signal owing to the filter compensation.

In this paper, a command-filtered adaptive backstepping control for photovoltaic grid-connected inverter is designed to control the DC link voltage and the injection of active and reactive power. At the same time, Lyapunov stability theory is used to prove that the control system can be maintained asymptotically stable.

2. **Grid-Connected Photovoltaic Inverter Model.** Figure 1 represents a topical three-phase grid-connected PV inverter system, which includes a PV array, a DC link filter capacitor C, a three-phase inverter, an output filter inductor L, and a three-phase grid.

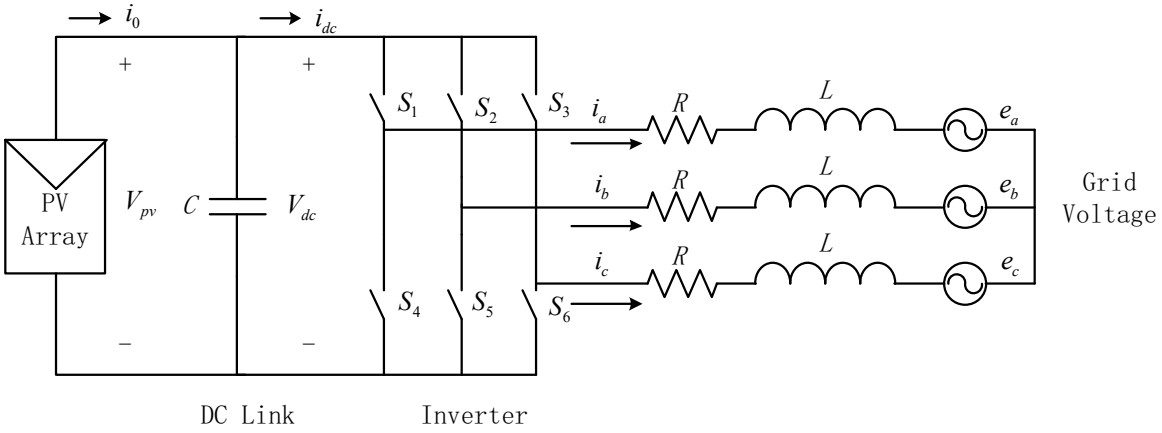

FIGURE 1. Three-phase grid-connected PV inverter system

In the original three-phase *abc* frame, the dynamic model of the grid-connected inverter system can be represented through the following functions [2]:

$$\begin{aligned} L\frac{di_a}{dt} &= -Ri_a - e_a + \frac{v_{dc}}{3}(2S_a - S_b - S_c) \\ L\frac{di_b}{dt} &= -Ri_b - e_b + \frac{v_{dc}}{3}(-S_a + 2S_b - S_c) \\ L\frac{di_c}{dt} &= -Ri_c - e_c + \frac{v_{dc}}{3}(-S_a - S_b + 2S_c) \end{aligned} \tag{1}$$

where the symbols of their usual meaning are showed in [4] and S_a, S_b and S_c represent the input switching signals. It is important to note that the model (1) is time varying and nonlinear. Here, with the *dq* transformation, the time-varying model becomes constant.

Finally, the dynamics of current in the *dq* frame can be shown as follows:

$$\begin{aligned} \frac{di_d}{dt} &= -\frac{R}{L}i_d + \omega i_q - \frac{E_d}{L} + \frac{v_{dc}}{L}S_d \\ \frac{di_q}{dt} &= -\frac{R}{L}i_q - \omega i_d - \frac{E_q}{L} + \frac{v_{dc}}{L}S_q \end{aligned} \tag{2}$$

where i_d, i_q are the d- and q-axis grid currents, respectively; E_d and E_q are the d- and q-axis grid voltages, respectively; S_d, S_q are the d- and q-axis switching functions, respectively. According to the KCL, the relationship of DC link voltage can be written as:

$$C\frac{du_{dc}}{dt} = i_0 - i_{dc} \tag{3}$$

where u_{dc} is the DC link voltage, i_{dc} is the current at the input of the inverter; i_0 is the current at the output of the solar array. In the synchronous rotating *dq*-frame, the active

and reactive powers exchanged between the PV array and the grid are given by:

$$\begin{aligned} P &= \frac{3}{2}\left(E_d I_d + E_q I_q\right) \\ Q &= \frac{3}{2}\left(E_q I_d - E_d I_q\right) \end{aligned} \tag{4}$$

However, in steady-state, the average value of E_q is equal to zero. And also, considering that the losses due to switching actions of the inverter are negligible, the power balance relationship is $u_{dc} i_0 = 1.5 E_d I_d$. Thus, the DC link voltage dynamics is expressed by:

$$\frac{du_{dc}}{dt} = \frac{3E_d I_d}{2CU_{dc}} - \frac{i_{dc}}{C} \tag{5}$$

Now considering the uncertainty of the model parameters and the uncertainty caused by the grid disturbance, the complete dynamical model of a grid-connected photovoltaic inverter system can be described by:

$$\begin{aligned} \frac{du_{dc}}{dt} &= \frac{3E_d i_d}{2Cu_{dc}} - \frac{i_{dc}}{C} + \delta_1 \\ \frac{di_d}{dt} &= -\frac{R}{L} i_d + \omega i_q - \frac{E_d}{L} + \frac{u_d}{L} + \delta_2 \\ \frac{di_q}{dt} &= -\frac{R}{L} i_q - \omega i_d - \frac{E_q}{L} + \frac{u_q}{L} + \delta_3 \end{aligned} \tag{6}$$

where δ_1, δ_2 and δ_3 respectively represent the sum of the uncertain parts of the non-linear and external disturbances in the grid-connected inverter model.

3. **Adaptive Command-Filtered Backstepping Controller Design.** In this section, the controller of PV grid-connected inverter controlling DC voltage and active and reactive power is designed step by step as follows.

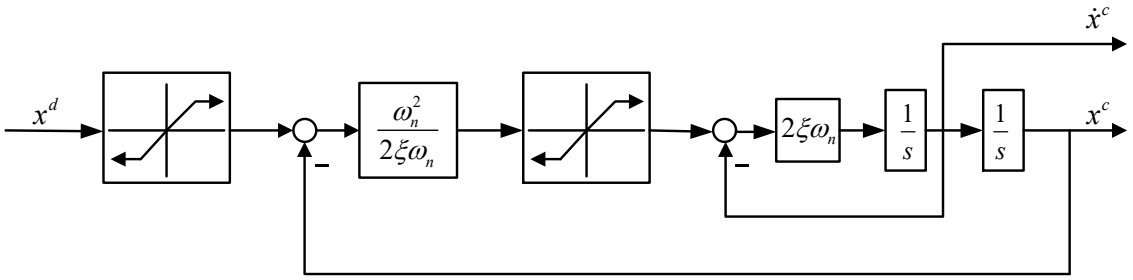

FIGURE 2. Structure of constrained command filter

Step 1. The tracking error variables e_1, e_2 and e_3 are defined as follows:

$$e_1 = u_{dc} - u_{dc}^c, \quad e_2 = i_d - i_d^c, \quad e_3 = i_q - i_q^c \tag{7}$$

where u_{dc}^c is the input reference voltage and i_d^c and i_q^c are the filtered command of i_d and i_q, correspondingly. The structure of command filter is shown in Figure 2.

Step 2. The task is to stabilize (7) and the Lyapunov function can be chosen as:

$$V_1 = \frac{1}{2} {e_1}^2 + \frac{\tilde{\delta}_1^2}{2\gamma_1} \tag{8}$$

where $\tilde{\delta}_1 = \hat{\delta}_1 - \delta_1$, $\hat{\delta}_1$ is the estimated value of δ_1, $\tilde{\delta}_1$ is the estimation error, γ_1 is adaptive gains.

Now the derivative of V_1 is given by:

$$\begin{aligned}\dot{V}_1 &= e_1\dot{e}_1 + \frac{\tilde{\delta}_1}{\gamma_1}\dot{\hat{\delta}}_1 \\ &= -k_1{e_1}^2 + e_1\left(\frac{3E_d i_d}{2Cu_{dc}} - \frac{i_{dc}}{C} + \hat{\delta}_1 - \dot{u}_{dc}^c + k_1 e_1\right) + \tilde{\delta}_1\left(\frac{\dot{\hat{\delta}}_1}{\gamma_1} - e_1\right)\end{aligned} \tag{9}$$

So the virtual controller can be considered as

$$\begin{aligned} i_d^d &= \frac{2Cu_{dc}}{3E_d}\left(\frac{i_{dc}}{C} - \hat{\delta}_1 + \dot{u}_{dc}^c - k_1 e_1\right) \\ \dot{\hat{\delta}}_1 &= \gamma_1 e_1\end{aligned} \tag{10}$$

where i_d^d is the desired velocity and $k_1 > 0$ is a design constant. Substituting (10) into (9), we have $\dot{V}_1 < 0$. Thus, based on Lyapunov stability theory, the virtual control is asymptotically stable.

In order to solve the problems of differential expansion and the control saturation, a command filter is used to eliminate the impact of time derivative of (11) and control saturation. Passing i_d^d through a filter, which is shown in Figure 2, the state-space model of command filter can be described as

$$\left\{\begin{array}{c} \dot{q}_1 \\ \dot{q}_2 \end{array}\right\} = \left[\begin{array}{c} q_2 \\ 2\xi\omega_n\left[S_R\left(\frac{{\omega_n}^2}{2\xi\omega_n}\right)(S_M(u) - q_1) - q_2\right] \end{array}\right] \tag{11}$$

where

$$\left\{\begin{array}{c} q_1 \\ q_2 \end{array}\right\} = \left[\begin{array}{c} x^c \\ \dot{x}^c \end{array}\right], \quad u = x^d \tag{12}$$

And ξ and ω_n are the damping and the bandwidth of the filter, respectively.

It is worth noting that the command filter will produce a filtering error which may increase the difficulty in getting the tiny tracking error. So we redefine tracking error $\bar{e}_1 = e_1 - \varepsilon_1$, and design compensating signals given by

$$\dot{\varepsilon}_1 = -k_1\varepsilon_1 + \frac{3E_d}{2Cu_{dc}}\left(i_d^c - i_d^d\right) \tag{13}$$

Step 3. To stabilize the second and the third functions of (7), the following Lyapunuov function is considered to obtain:

$$V_2 = \frac{1}{2}\left(\bar{e}_1^2 + {e_2}^2 + {e_3}^2 + \frac{\tilde{\delta}_2^2}{\gamma_2} + \frac{\tilde{\delta}_3^2}{\gamma_3}\right) \tag{14}$$

where $\tilde{\delta}_2 = \hat{\delta}_2 - \delta_2$, $\tilde{\delta}_3 = \hat{\delta}_3 - \delta_3$, γ_2 and γ_3 are another two adaptive gains.

According to (8), (11) and (14), the derivative equation for $\dot{\bar{e}}_1$ is calculated as

$$\dot{\bar{e}}_1 = \frac{3E_d i_d}{2Cu_{dc}} - \frac{i_{dc}}{C} + \delta_1 - \dot{u}_{dc}^c + k_1\varepsilon_1 - \frac{3E_d}{2Cu_{dc}}\left(i_d^c - i_d^d\right) = \frac{3E_d}{2Cu_{dc}}e_2 - \tilde{\delta}_1 - k_1\bar{e}_1 \tag{15}$$

Then, we can compute the derivative of V_2:

$$\begin{aligned}\dot{V}_2 &= \bar{e}_1\dot{\bar{e}}_1 + e_2\dot{e}_2 + e_3\dot{e}_3 + \frac{\tilde{\delta}_2}{\gamma_2}\dot{\hat{\delta}}_2 + \frac{\tilde{\delta}_3}{\gamma_3}\dot{\hat{\delta}}_3 \\ &= -k_1\bar{e}_1^2 - k_2{e_2}^2 - k_3{e_3}^2 - \bar{e}\tilde{\delta}_1 \\ &\quad + e_2\left(\frac{3E_d}{2Cu_{dc}}\bar{e}_1 - \frac{R}{L}i_d + \omega i_q + \frac{u_d - E_d}{L} + \hat{\delta}_2 - \dot{i}_d^c + k_2 e_2\right)\end{aligned}$$

$$
\begin{aligned}
&+ e_3\left(-\frac{R}{L}i_q - \omega i_d + \frac{u_q - E_q}{L} + \hat{\delta}_3 - \dot{i}_q^c + k_3 e_3\right) \\
&+ \tilde{\delta}_2\left(\frac{\dot{\hat{\delta}}_2}{\gamma_2} - e_2\right) + \tilde{\delta}_3\left(\frac{\dot{\hat{\delta}}_3}{\gamma_3} - e_3\right)
\end{aligned} \tag{16}
$$

where $k_2 > 0$ and $k_3 > 0$ are the design constants. And we choose the virtual control u_d and u_q as:

$$
\begin{aligned}
u_d &= -L\left(\frac{3E_d}{2Cu_{dc}}\bar{e}_1 - \frac{R}{L}i_d + \omega i_q - \frac{E_d}{L} + \hat{\delta}_2 - \dot{i}_d^c + k_2 e_2\right) \\
u_q &= -L\left(-\frac{R}{L}i_q - \omega i_d - \frac{E_q}{L} + \hat{\delta}_3 - \dot{i}_q^c + k_3 e_3\right) \\
\dot{\hat{\delta}}_2 &= \gamma_2 e_2 \\
\dot{\hat{\delta}}_3 &= \gamma_3 e_3
\end{aligned} \tag{17}
$$

Then we will get

$$
\dot{V}_2 = -k_1\bar{e}_1^2 - k_2 {e_2}^2 - k_3 {e_3}^2 - \bar{e}\tilde{\delta}_1 < 0 \tag{18}
$$

For sufficiently large k_1, k_2 and $k_3 > 0$, thus, it is proven that the whole system is asymptotically stable.

4. **Simulation Results.** In this section, the Matlab/Simulink has been used for simulating the proposed control. The parameters of the model used in the dynamic simulation are summed in Table 1. In addition, the reference power changes its value as follows: 0 kw from the time $t = 0$ s, 8 kw from the time $t = 0.06$ s, 0.6 kVar from the time $t = 0.2$ s, 5 kw from the time $t = 0.3$ s, 0.3 kVar from the time $t = 0.5$ s, and 10 kw from the time $t = 0.6$ s. As illustrated by Figure 3, the active and reactive powers closely track to its desired value. Meanwhile, Figure 4 represents that the DC link voltage V_{dc} is regulated to the set value $V_{ref} = 200$ V. And also, Figure 4 displays the changes of the grid current with the grid voltage.

Table 1. Parameters of the system

Parameter	Representation	Value
C (μF)	DC link capacitor	2800
R (Ω)	Filter resistances	0.1
L (mH)	Filter inductor	20
V_{dc}^{ref} (V)	Desired DC link voltage	200
V_g (V)	Grid voltage	110
F (Hz)	Grid frequency	50

5. **Conclusion.** In this paper, a new recursive method to control the active and reactive power injection into the grid from a three-phase grid-connected PV system is proposed. The proposed controller is designed considering all parameters of the system as unknown and these unknown parameters are estimated through the adaptation laws. From the simulation results, it is clear that the designed nonlinear adaptive backstepping controller provides a very satisfactory performance in terms of maintaining steady-state operation under various operating conditions as compared to the value of reference and the robustness against the parameter uncertainties and the time-varying external disturbances. Future work will study the design of similar controllers by taking into account of unknown parameters. Future work will also focus on estimation of unknown parameters of interconnected systems with multiple photovoltaic arrays.

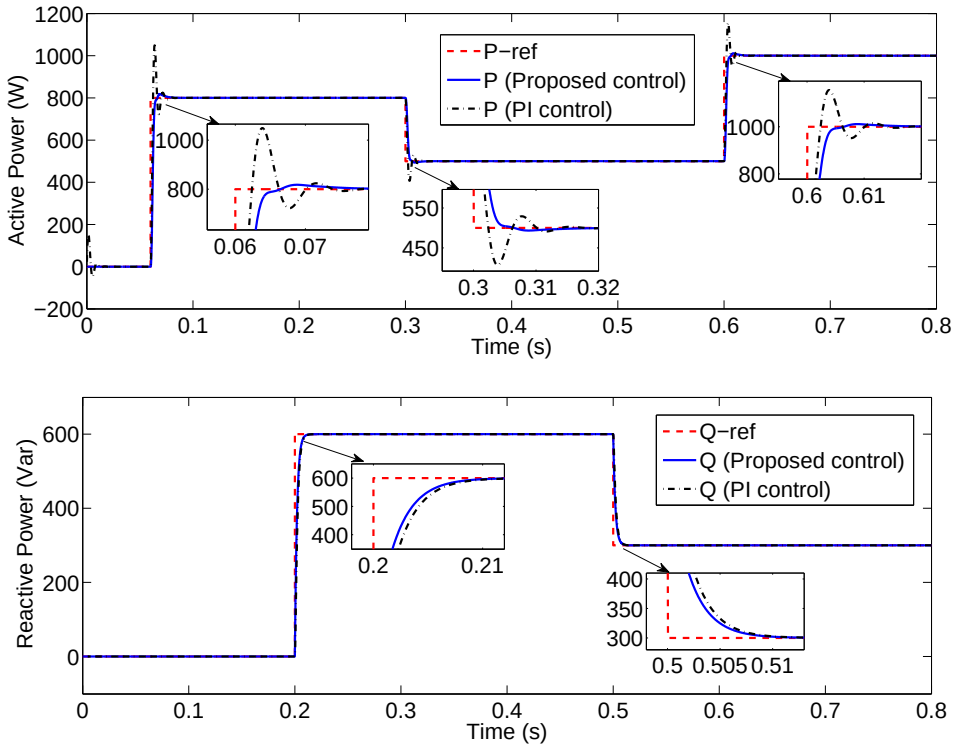

FIGURE 3. Active and reactive power injected into the grid

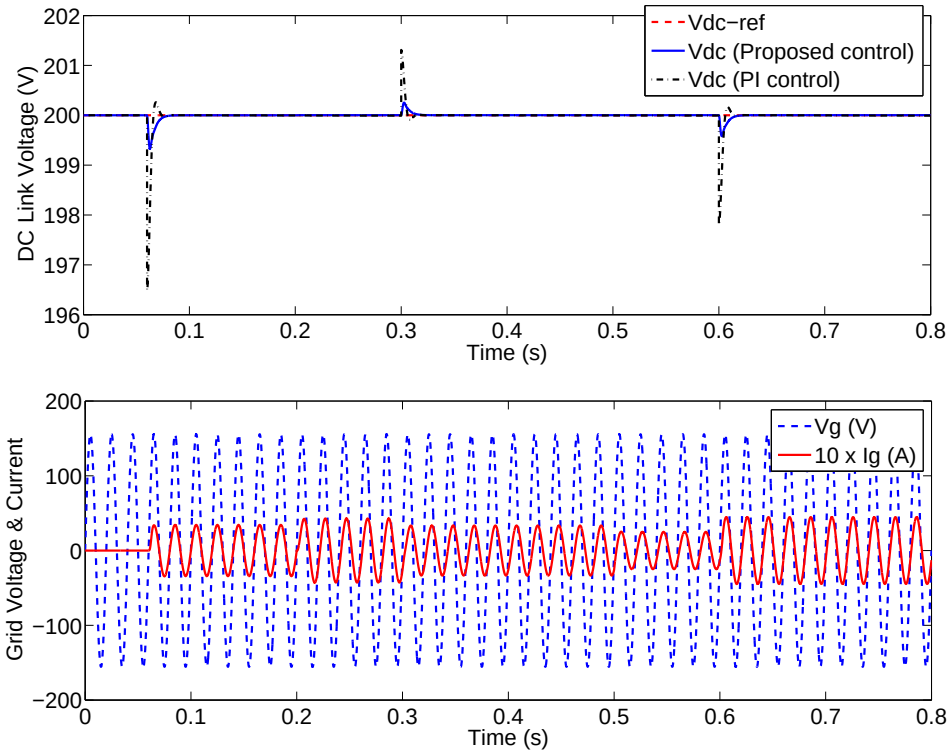

FIGURE 4. DC link voltage and grid voltage and current

Acknowledgment. This work is supported by National Natural Science Foundation of China (61503156, 51405198), the Fundamental Research Funds for the Central Universities (JUSRP11562, JUSRP51406A, and NJ20150011), National Key Research and Development Program (2016YFD0400300) and the Science and Technology Funds for Jiangsu China (BY2015019-24).

REFERENCES

[1] K. M. Tsang and W. L. Chan, Three-level grid-connected photovoltaic inverter with maximum power point tracking, *Energy Conversion and Management*, vol.65, pp.221-227, 2013.

[2] A. Kotsopoulos, J. L. Duarte and M. A. M. Hendrix, Predictive DC voltage control of single-phase PV inverters with small DC link capacitance, *IEEE Int. Symposium on Industrial Electronics*, vol.2, pp.793-797, 2003.

[3] I.-S. Kim, Sliding mode controller for the single-phase grid-connected photovoltaic system, *Solar Energy*, vol.83, no.10, pp.1101-1115, 2006.

[4] M. A. Mahmud, H. Pota and M. J. Hossain, Nonlinear current controller scheme for a single-phase grid-connected photovoltaic system, *IEEE Trans. Sustainable Energy*, vol.5, no.1, pp.218-227, 2014.

[5] A. E. Fadili, F. Giri and A. E. Magri, Reference voltage optimizer for maximum power point tracking in triphase grid-connected photovoltaic systems, *Int. Journal of Electrical Power and Energy Systems*, 2014.

[6] F. Mazenc and P.-A. Bliman, Backstepping design for time-delay nonlinear systems, *IEEE Trans. Automatic Control*, vol.51, no.1, pp.149-154, 2006.

[7] Z.-Y. Sun, T. Li and S.-H. Yang, A unifed time-varying feedback approach and its applications in adaptive stabilization of high-order uncertain nonlinear systems, *Automatica*, vol.70, no.8, pp.249-257, 2016.

[8] J. Yu, P. Shi, W. Dong, B. Chen and C. Lin, Neural networkbased adaptive dynamic surface control for permanent magnet synchronous motors, *IEEE Trans. Neural Networks and Learning Systems*, vol.26, no.3, pp.640-645, 2015.

[9] W. Dong, J. A. Farrell, M. M. Polycarpou, V. Djapic and M. Sharma, Command filtered adaptive backstepping, *IEEE Trans. Control Systems Technology*, vol.20, no.3, pp.566-580, 2012.

[10] J. A. Farrell, M. Polycarpou, M. Sharma and W. Dong, Command filtered backstepping, *IEEE Trans. Automatic Control*, vol.54, no.6, pp.1391-1395, 2009.